Progress In Electromagnetics Research Letters, Vol. 20, 27–36, 2011

LARGE SIGNAL EQUIVALENT CIRCUIT MODEL FOR PACKAGE ALGaN/GaN HEMT

L. Sang, Y. Xu, Y. Chen, Y. Guo, and R. Xu

EHF Key Laboratory of Fundamental Science
University of Electronic Science and Technology of China
Chengdu 611731, China

Abstract—In this paper, a large signal equivalent circuit empirical model based on Anglov model for ceramic package high power AlGaN/GaN HEMT has been proposed. A temperature-dependent drain current model, including self-heating effect, has been presented, and good agreements are achieved between measurement results and calculated results at different temperatures. The nonlinear capacitance models are modeled directly by measured microwave scattering (S) parameters and multi-bias small signal equivalent circuit model (SSECM) of package device is also established based on the measurements. A power amplifier based on large size AlGaN/GaN HEMT with a total gate periphery of 36 mm has been designed by using the proposed model for validation purpose, and the simulation results fit the measurement results well at different temperatures.

1. INTRODUCTION

Recently, AlGaN/GaN HEMT is emerging as a frequently employed technology in high power RF devices due to high maximum cut-off frequency (f_T), high breakdown voltage, high power density and high operating temperature [1]. Accurate large signal model is crucial for GaN power devices and circuit design. Compared with physical based model [2] and table based empirical model [3], empirical large signal equivalent circuit model (LSECM) is more simple and easier to be implemented in microwave commercial simulation software, and has been widely used in GaAs and SiC based devices [4, 5]. However, accurate LSECM for GaN based devices is still a major topic of

Received 7 November 2010, Accepted 5 January 2011, Scheduled 16 January 2011
Corresponding author: Lei Sang (sanglei2008@126.com).

discussion due to the existence of thermal effects and trapping related dispersion in GaN HEMT devices [2, 3, 6, 7]. A common way to build the LSECM starts from small gate periphery GaN HEMT, and extends it into application of large gate periphery or even multi-cell large size devices by using scalable technique. Because the measurements of microwave scattering (S) parameter are less affected by self-heat effect and the output power character can be easily measured by using load pull measurement for small size device, this method can obtain accurate LSECM for small gate periphery GaN HEMT. However, the accuracy of LSECM is largely limited when it extends to large size device due to the inhomogeneous of heat transportation and trapping distribution induced by processing [8]. Moreover, the prediction performance of package device based on LSECM developed from small size device will become worse duo to the parasitic parameters effect and heat transportation in ceramic cavity.

In this paper, an empirical LSECM for large gate periphery package AlGaN/GaN HEMT device has been developed based on bottom-up technology. A small signal equivalent circuit model (SSECM) is established directly by measured S parameters of package device at different biases [9], and the nonlinear capacitance models are empirically modeled based on multi-bias SSECM. The nonlinear drain-source current ($I-V$) model is modeled by fitting with measured $I-V$ curve accounting thermal effect.

The thickness of the silicon carbide (SiC) substrate of the device is 150 µm. The T shape gate is made from Ni/Au with 0.5 µm width. The SiNx is used as passivation and encapsulation layer. The whole device contained 18 cells and the gate periphery for each cell is 2 mm, and is packed with ceramic. In band below 3.8 GHz the device could operates normally.

2. SMALL-SIGNAL EQUIVALENT CIRCUIT MODEL

In order to include the package effect of large gate periphery device, the parasitic parameters should be taken good consideration for high frequency application. Jarndal and Kompa [10] have studied the 22-elements distributed topology and extraction method for AlGaN/GaN HEMT, and Lu et al. [11] proposed a 20-elements topology and extraction method for AlGaN/GaN HEMT. In this paper, we use a compact model with 19 elements as shown in Fig. 1. The parasitic parameters include parasitic inductances and resistances at source (L_s and R_s), drain(L_d and R_d), and gate (L_g and R_g) electrodes, parasitic capacitors between gate to source (C_{gsi}), gate to drain (C_{gdi}), and drain to source (C_{dsi}), as well as parasitic capacitors (C_{pg} and C_{pd}) induced

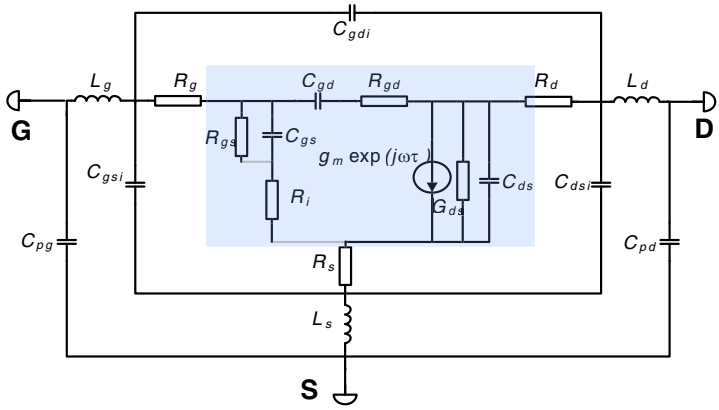

Figure 1. 19-elements GaN HEMT SSECM.

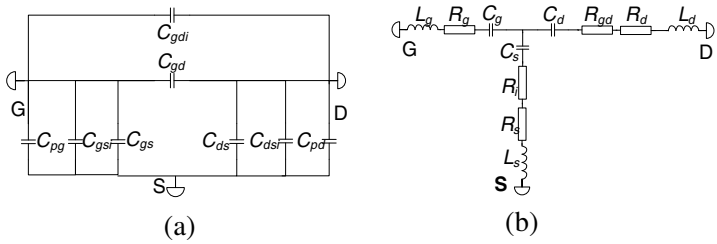

Figure 2. (a) Equivalent circuits for cold pin-off and (b) unbiased condition.

by package effect. The effects of parasitic capacitor between gate and drain induced by package effect and parasitic parallel resistance between gate and drain are very small and can be negligible if the operation frequency less than 10 GHz, so we ignore them to simplify the parameters extraction method.

Considering the complexity of SSECM, the cold FET method is used to give a few relationships between parasitic parameters before extracting the intrinsic parameters. The equivalent circuit of cold FET with pinch-off bias at low frequencies (< 500 MHz) can be simplified (shown in Fig. 2(a))and the Y-parameters of the equivalent circuit can be written as:

$$\mathrm{Im}(Y_{11}) = j\omega(C_{pg} + C_{gsi} + C_{gs} + C_{gdi} + C_{gd}) \quad (1)$$

$$Im(Y_{12}) = -j\omega(C_{gdi} + C_{gd}) \quad (2)$$

$$Im(Y_{22}) = j\omega(C_{pd} + C_{dsi} + C_{ds} + C_{gdi} + C_{gd}) \quad (3)$$

where, $\omega = 2\pi f$ is the angular frequency. At high frequencies

($f > 10\,\mathrm{GHz}$) the equivalent circuit for unbiased FET is shown in Fig. 2(b). The Z-parameter can be written as:

$$Z_{11} = R_g + R_i + R_s + j\omega\,(L_g + L_s) + \frac{1}{j\omega}\left(\frac{1}{C_g} + \frac{1}{C_s}\right) \tag{4}$$

$$Z_{12} = R_i + R_s + j\omega L_s + \frac{1}{j\omega C_s} \tag{5}$$

$$Z_{22} = R_d + R_i + R_s + R_{gd} + j\omega(L_s + L_d) + \frac{1}{j\omega}\left(\frac{1}{C_d} + \frac{1}{C_s}\right) \tag{6}$$

The optimization algorithm based method is adopted to determine all the parameters due to the large number of unknown parameters in Eq. (1)–Eq. (6), First, the parasitic inductances L_g, L_s, L_d can be calculated by the slopes of straight lines interpolating the experimental data of the imaginary parts of the Z-parameters multiplied by the angular frequency ω versus ω^2. $C_{pg} = aC_{gsi} = bC_{gs}$, $C_{pd} = cC_{dsi} = dC_{ds}$, $C_{gd} = eC_{gdi}$, $R_i = xR_{gd}$ and $R_g = gR_d$ are defined based on the geometry of device. Then, the Y-parameters of intrinsic (Y_{int}) elements could be extracted after eliminating the effect of the parasitic parameters [12–14]. Finally, the optimization algorithm is used to extract all parameters. In order to improve the optimization efficiency and accuracy, the optimization ranges and steps of the seven ratio parameters (a, b, c, d, e, x, g) are set to reasonable values. The simple genetic algorithm (GA) is used as the optimization algorithm [15]. The extracted parameters are shown in Table 1, and good agreements are achieved between measurement results and calculated results (shown in Fig. 3).

Table 1. The calculated parameters (capacitances in fF, inductances in nH, resistances in Ohm, and conductance in mS) for 36 mm gate periphery AlGaN/GaN HEMT.

C_{pg}	C_{gsi}	C_{gs}	C_{pd}	C_{dsi}	C_{ds}	C_{gd}	C_{gdi}	L_g	L_s	L_d
0.09	10.94	0.86	1.29	0.17	0.10	0.10	0.11	0.45	0.17	4.49
R_g	R_d	R_s	R_{gs}	R_i	R_{gd}	G_{ds}	g_m	τ	a	b
7.09	26.07	1.10	12.00 k	0.47	1.84	0.83	278.00	1.20 ns	0.92	11.65
c	d	e	x	g						
7.87	12.49	0.97	0.26	0.27						

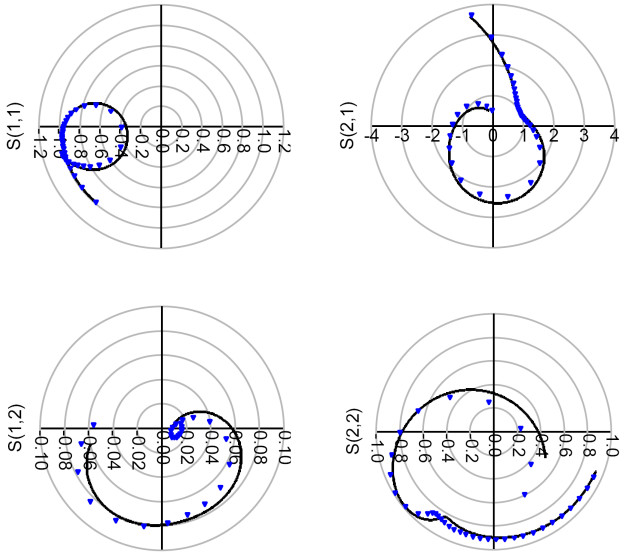

Figure 3. Comparisons of calculated (solid line) and measured S-parameters (triangle line) at $V_{gs} = -1.4\,\mathrm{V}$, $V_{ds} = 28\,\mathrm{V}$ in the frequency range from 0.1 GHz to 4.5 GHz.

3. LARGE-SIGNAL EQUIVALENT CIRCUIT MODEL

Figure 4 shows the AlGaN/GaN HEMT large-signal equivalent circuit topology. Typically, there are three main nonlinear elements: source-drain current (I_{ds}), gate-source capacitor (C_{gs}), and gate-drain capacitor (C_{gd}). A modified I_{ds} model based on the Angelov model is presented

$$I_{ds} = I_{pk}(1 + \tanh(f_1))(1 + f_2 V_{ds}) \tanh(DV_{ds}) \tag{7}$$

$$f_1 = p_1(V_{gs} - v_{pk}) + p_2(V_{gs} - v_{pk})^2 + p_3(V_{gs} - v_{pk})^3 \tag{8}$$

$$I_{pk} = \frac{I_{pk0}}{A(V_{ds}^p V_{gs}^q) + BV_{ds}^{0.6V_{gs}} + C} \times \frac{K}{\exp(\frac{T-300}{200})} \tag{9}$$

$$v_{pk} = F + GV_{ds} \tag{10}$$

$$f_2 = H \exp\left(M\,|V_{gs}|^Q\right) \tag{11}$$

where, V_{ds} is the drain to source voltage; V_{gs} is the gate to source voltage; I_{pk} is the saturation current and V_{pk} is the knee voltage; A, B, C, D, p_1, p_2, and p_3 are constants; F and G are used to describe the V_{ds} effect on knee voltage caused by short-channel effects. Compared with Angelov model, two main modifications have been added:

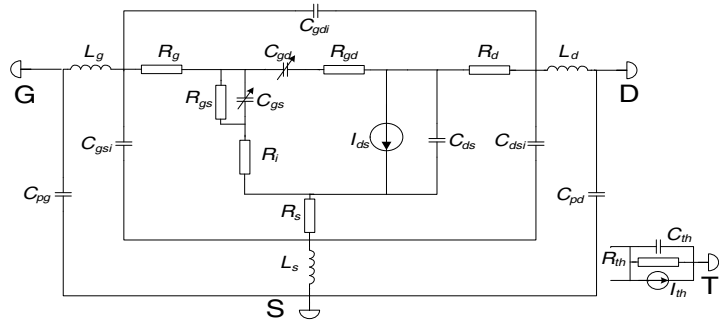

Figure 4. AlGaN/GaN HEMT large-signal equivalent circuit topology.

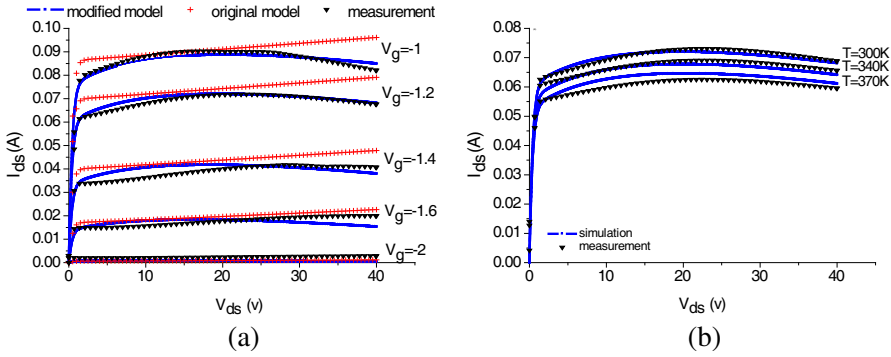

Figure 5. For (a) Comparison between calculated $I - V$ results by using modified model and original model and measurement date on one cell device ($T = 300\,\mathrm{K}$). For (b) $I - V$ curve at different ambient temperatures on one cell ($V_{gs} = -1.2\,\mathrm{V}$).

a) Self-heating effect. The saturation current decreases duo to the self-heating effect at high bias current, so an compact expression (term including A, B, and C) is added to the denominator of Eq. (9).

b) Temperature dependent effect. T represents the ambient temperature, and K is a correction factor.

Due to the large effect of self-heat and ambient temperature, a small gate periphery device (one cell with 2 mm gate width) is measured and used to validate the proposed model. Fig. 5(a) shows the comparisons of calculated and measured results, and a good agreement has been achieved with consideration of self-heat effect. Fig. 5(b) shows the calculated I_{ds} at different T. The results show that even with good

thermal conductivity of AlGaN/GaN HEMT, the self-heat effect and ambient temperature still have important effects on the performance of the device.

The modified model of C_{gs} and C_{gd} based on Angelov model are given below:

$$f_{ai1} = M_1 + P_{11} * v_{gs} + P_{111} * \frac{|v_{gs}|}{10 * v_{ds}} \tag{12}$$

$$f_{ai2} = M_2 * v_{gs} + P_{21} * \left(M_{21} + v_{gs} + \frac{|v_{gs} * v_{ds}|}{10} \right) \tag{13}$$

$$C_{gs} = C_{gs0} + C_{gs0} * (1 + \tanh(f_{ai1})) * (1 + \tanh(f_{ai2})) \tag{14}$$

where, V_{gs} and V_{ds} are both added to f_{ai1} and f_{ai2} in order to express the dual modulation effect of channel.

$$C_{gd} = N_1 + N_2 * (1 + \exp(N_3 * v_{gs} + N_4)) * \exp(N_5 * v_{ds}) \tag{15}$$

where, the exponent function is used instead of hyperbolic tangent function. Fig. 6 shows the comparison of calculated results and measured results based on multi-bias SSECM.

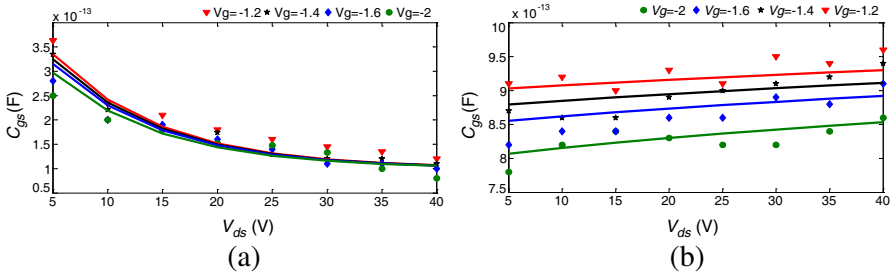

Figure 6. The fitting curve (solid line) for the (a) C_{gs} and (b) C_{gd} extracted from small-signal model based on measurement dates (triangle).

4. POWER AMPLIFIER CIRCUIT DESIGN

The LSECM is implemented in Advanced Design System (ADS) by using symbolic defined devices (SDD). The parasitic parameters are keeping constant extracted from SSECM. In the design of the power amplifier, the frequency range is from 3.3 GHz to 3.8 GHz and the bias conditions are chosen at $V_{gs} = -1.4$ V and $V_{ds} = 28$ V, which is typical operation bias for class A in the device. By comprehensive consideration of stability, gain and maximum power output, the input

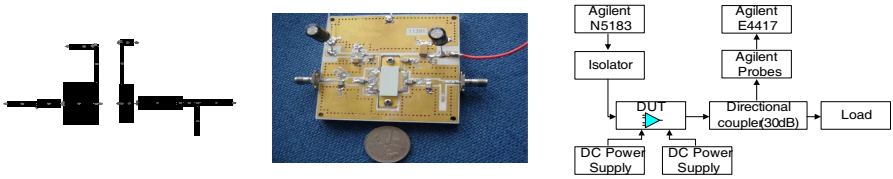

(a) (b) (c)

Figure 7. Schematic of input/output matching of (a) the power amplifier circuit, (b) the final power amplifier, and (c) measurement setup for power amplifier.

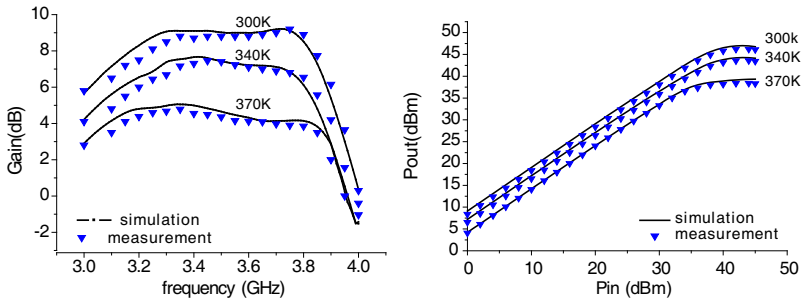

(a) (b)

Figure 8. Gain and Output power characteristic between simulation results and measurements at different ambient temperatures biased at $V_{gs} = -1.4\,\mathrm{V}$ and $V_{ds} = 28\,\mathrm{V}$ (for (a) input power $P_{in} = 20\,\mathrm{dBm}$, for (b) $f = 3.7\,\mathrm{GHz}$).

impedance is set to $5.8 + j * 0.5$ and the output impedance is set to $6.1 - j * 14.4$. The impedance matching circuits are shown in Fig. 7(a), and the final circuit is made on the substrate of ROGERS 4350 [16, 17].

The measurement setup of the power amplifier (DUT) is shown in Fig. 7(c). The input signal was supplied by Agilent N5183 microwave analog signal generator cascaded by an isolator. The output of the amplifier was measured by directional coupler and power meter Agilent E4417. Figs. 8(a) and (b) show the simulated gain and output power characteristic by using proposed LSECM model at different temperatures, respectively. And the results fit the measurements well. In the interested frequency band, the linear gain for the amplifier is about 8.5 dB at 300 K with 46 dBm output power, and they decrease dramatically when ambient temperature go up to more than 350 K.

5. CONCLUSION

A LSECM for package large size AlGaN/GaN HEMT is established in this paper. The self-heat and temperature effect are considered in $I - V$ model, and the nonlinear capacitors are extracted from 19 elements SSECM and directly used in multi-bias measurement of large gate periphery device. An amplifier is designed by using the proposed model for validation purpose, and the results show that the simulated results fit the measurements well. The proposed model can be used to analysis temperature effect on AlGaN/GaN power HEMT and design high power GaN HEMT amplifier.

ACKNOWLEDGMENT

Thanks go to our friend from the 38th research institute of China Electronics Technology Group Corporation (CETC-38), who has given great support on the study. This work is supported by National Science Foundation of China part under Grant 60701017 and part under Grant 60876052.

REFERENCES

1. Mishra, U. K., L. Shen, T. E. Kazior, and Y.-F. Wu, "GaN-based RF power devices and amplifiers," *Proc. of the IEEE*, Vol. 96, No. 2, 287–305, Feb. 2008.
2. Mari, D., M. Bernardoni, G. Sozzi, et al., "A physical large-signal model for GaN HEMTs including self-heating and trap-related dispersion," *Microelectronics Reliability*, Oct. 16, 2010.
3. Jarndal, A., et al., "Large-signal model for AlGaN/GaN HEMTs suitable for RF switching-mode power amplifiers design," *Solid-state Electronics*, Vol. 54, No. 7, 696–700, Jul. 2010.
4. Angelov, I., V. Desmaris, K. Dynefors, P. A. Nilsson, N. Rorsman, and H. Zirath, "On the large-signal modeling of AlGaN/GaN HEMTs and SiC MESFETs," *Gallium Arsenide and Other Semicond. Appl. Symp.*, 309–312, Oct. 2005.
5. Xu, Y., Y. Guo, R. Xu, B. Yan, and Y. Wu, "An support vector regression based nonlinear modeling method for SiC MESFET," *Progress In Electromagnetics Research Letter*, Vol. 2, 103–114, 2008.
6. Yuk, K. S., G. R. Branner, and D. J. McQuate, "A wideband multiharmonic empirical large-signal model for high-power GaN HEMTs with self-heating and charge-trapping effects," *IEEE*

Transactions on Microwave Theory and Techniques, Vol. 57, No. 12, 3322–3332, Dec. 2009.

7. Jardel, O., F. de Groote, T. Reveyrand, et al., "An electrothermal model for AlGaN/GaN power HEMTs including trapping effects to improve large-signal simulation results on high VSWR," *IEEE Transactions on Microwave Theory and Techniques*, Vol. 55, No. 12, 2660–2669, Dec. 2007.
8. Dahmani, S., E. S. Mengistu, and G. Kompa, "Electrothermal modeling of large-size GaN HEMTs," *German Microwave Conference (GeMIC)*, 2008.
9. Tajima, Y., "100 W GaN HEMT modeling," *Microwave Journal*, May 2007.
10. Jarndal, A. and C. Kompa, "An accurate small-signal model for AlGaN-GaN HEMT suitable for scalable larger-signal model construction," *IEEE Microwave Wireless Components Letter*, Vol. 16, No. 6, 333–335, Jun. 2006.
11. Lu, J., Y. Wang, L. Ma, and Z. Yu, "A new small-signal modeling and extraction method in AlGaN/GaN HEMTs," *Solid-state Electronics*, Vol. 52, No. 1, 115–120, Jan. 2008.
12. Khalaf, Y. A., "Systematic optimization technique for MESFET modeling," Doctor Dissertation, Virginia Polytechnic Institute and State University, 2000.
13. Gao, J., X. Li, H. Wang, and G. Boeck, "A new method for determination of parasitic capacitances for PHEMTs," *Semicond. Sci. Technol.*, Vol. 20, 586–591, 2005.
14. Qian, F., J. H. Leach, and H. Morkoc, "Small signal equivalent circuit modeling for AlGaN/GaN HFET: Hybrid extraction method for determining circuit elements of AlGaN/GaN HFET," *Proceedings of the IEEE*, Vol. 98, No. 7, Jul. 2010.
15. Xu, Y., Y. Guo, R. Xu, B. Yan, and Y. Wu, "An improved small-signal equivalent circuit model for 4H-SiC power MESFETs," *Microw. and Opt. Techn. Lett.*, Vol. 50, No. 2, 1455–1458, 2008.
16. Jimenez Martin, J. L., V. Gonzalez-Posadas, J. E. Gonzalez-Garcia, F. J. Arques-Orobon, L. E. Garcia Munoz, and D. Segovia-Vargas, "Dual band high efficiency class e power amplifier based on CRLH diplexer," *Progress In Electromagnetics Research*, Vol. 97, 217–240, 2009.
17. Zhang, B., Y.-Z. Xiong, L. Wang, S. Hu, T.-G. Lim, Y.-Q. Zhuang, and L.-W. Li, "A d-band power amplifier with 30-GHz bandwidth and 4.5 dBm P_{sat} for high-speed communication system," *Progress In Electromagnetics Research*, Vol. 107, 161–178, 2010.